

Analysis, Design, Construction, and Testing of Deep Foundations

**Proceedings
of the OTRC '99
Conference**

**Geotechnical Special
Publication No. 88**

Edited by Jose M. Roesset



ASCE

pile tip to determine the end-bearing capacity. This value gives usually higher capacity than the undrained shear strength of undisturbed soil as in the case of soft cohesive soils especially for long piles.

ACKNOWLEDGMENTS

Part of this research was financially supported by The U.S. Department of Transportation, Federal Highway Administration Grant No. DTFH61-96-X-00002 through the project supported "Including All Deep Foundation Load Test Data and Soil and Site Investigations for the FHWA Database." The encouragement and support of Albert DiMillio, Carl Ealy, and Raghu Satyanarayana, Turner-Fairbank Highway Research Center, FHWA, are gratefully acknowledged. The assistance of J. B. Esnard and Ed Tavera, LA DOTD Pavement and Geotechnical Design Section, in getting pile load reports from department files is appreciated. Mrs. Elizabeth Hood, Department of Civil and Environmental Engineering - LSU, invested a great effort in the development of the pile load test database.

DISCLAIMER

The contents of this paper reflect the views of the authors who are responsible for the facts and the accuracy of the data presented herein. The contents do not necessarily reflect the views or policies of the Louisiana Department of Transportation and Development, the Louisiana Transportation Research Center, or the Federal Highway Administration. This paper does not constitute a standard, specification, or regulation.

REFERENCES

- Butler, H. D., and Hoy, H. E. (1977). "The Texas Quick-Load Method for Foundation Load Testing- User's Manual," Report No. FHWA-IP-77-8.
- Davisson, M. T., (1972). "High Capacity Piles," Proceedings of Lecture Series on Innovation in Foundation Construction, American Society of Civil Engineers, ASCE, Illinois Section, Chicago, pp81-112.
- Tomlinson, M. J., (1980). *Foundation Design and Construction*, 4th Edition, Pitman Advanced Publishing Program.
- Tumay, M. T., and Titi, H. H. (1998). "Including All Deep Foundation Load Test Data and Soil and Site Investigations for the FHWA Database," Final Report, Submitted to the U.S. Department of Transportation/Federal Highway Administration, Grant No. DTFH61-96-X-00002, Louisiana Transportation Research Center, Baton Rouge, Louisiana, 65 pp. + CD-ROM.
- Zenon, G. K., Schnore, A. R., Carlo, T. A., and Baily, B. F. (1992) "Static Testing of Deep Foundations," Report No. FHWA-SA-91-042.

An Experiment with Statnamic Lateral Loading of a Drilled Shaft

Dan A. Brown¹

Abstract

A lateral loading test of a full scale drilled shaft foundation is described, for which the loading is applied using the statnamic device. This device produces a rapid lateral loading with a duration of around 0.1 seconds. In addition to measurements of load and displacement at the top of the shaft, the test shaft was instrumented with strain gauges and accelerometers. A simple method of interpretation of the statnamic loading is presented which provides a means of accounting for inertial and viscous damping effects as well as nonlinear soil resistance. The results of this test are compared similar drilled shafts at the site which were loaded with conventional static methods. All of the testing described was performed at the Auburn University National Geotechnical Experimentation Site (NGES) at Spring Villa, Alabama in a silty soil.

Introduction

In recent years the statnamic loading device has seen increased use as a means of conducting load tests on deep foundations, primarily in the axial direction. The statnamic operates on the principal of Newton's second law, $F=ma$; a large mass is launched off the foundation element with an acceleration of 20g's or so, thus producing a thrust against the foundation

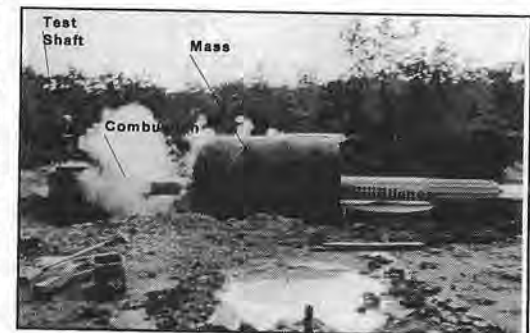


Figure 1 Statnamic Lateral Test

¹Gottlieb Assoc. Professor of Civil Engineering, Auburn University, AL 36849

which is 20 times the weight of the mass. The force to launch the mass is applied using combustion within a pressure chamber of a pelletized smokeless powder which burns at a very predictable rate.

This paper describes the use of a statnamic device to apply lateral loading to a deep foundation element, as illustrated on Figure 1. The mass is attached to a flat bottomed sled which slides away as the gas pressure builds and is seen in this figure just after the mass has separated from the piston and the exhaust gasses are venting. The statnamic loading produces a force which builds smoothly to a maximum and decays over a period of about 0.1 sec. This loading period represents a high rate of loading compared to conventional static testing, but is considerably slower than one which might be modeled using wave propagation techniques. Thus the test contains inertial and damping forces characteristic of a dynamic loading event, but has a load duration which is much longer than the typical natural period of the shaft. Such dynamic response may provide insight into the soil response which might be observed during large amplitude dynamic lateral loading events such as vessel impact or seismic loading.

The objective of this paper is to describe the results of one such lateral statnamic test on a drilled shaft foundation. This test shaft was carefully instrumented to provide measurement data important to understanding the performance of the foundation during such a loading event. The test was performed at the Auburn University NGES site, a location which has well documented soil material properties and conventional static lateral load tests which provide a basis for comparison. A total of four lateral statnamic tests were performed, and the response at the top of the shafts were similar; the test described in this paper represents the most well-instrumented shaft.

Soil Conditions

The soils at the test site are composed of a residual soil of decomposed gneiss and quartzite, typical of the Piedmont region of the southeastern U.S. (Vinson and Brown, 1998). These soils are classified as predominantly clayey silts and silty clays (ML-CL) with occasional sand lenses. The weathering is more advanced within the upper 4 meters (which are of most relevance to the lateral test) and these soils tend to be have higher clay content than those at greater depth. Other than the near-surface weathering, the soils within the upper 15 m at the site are relatively uniform on a large scale; on a small scale these soils exhibit significant spatial variability. Groundwater at the time of testing was at a depth of approximately 4 m. Some average soil properties of the soils within the upper 4 meters are provided on Table 1.

Based upon 20 CIUC triaxial tests performed on samples from the 4 to 15 m depth range, these soils have an effective cohesion of 17 kPa and effective friction angle of 31°. The upper 4 m have somewhat higher clay content and are likely to exhibit somewhat higher cohesion (although effective stress strength parameters have not directly been measured for shallow soils).

Property	Average Value	Range
water content	34%	30 to 40%
plasticity index	8%	2 to 20%
std penetration test	11 blows/30cm (b/f)	8 to 16 b/f
cpt tip resistance, q_c	2.5 MPa	2 to 3 MPa
cpt friction ratio	6%	5 to 8%
pressuremeter modulus	8 MPa	6 to 11 MPa
dilatometer modulus	15 MPa	10 to 25 MPa
shear wave velocity	200 m/s	180 to 240 m/s
S_u from UU triaxial	90 kPa	40 to 150 kPa

Table 1 Soil Properties for 0 to 4 m Depth

Test Shaft

All of the test shafts were constructed as drilled and cast-in-place concrete shafts to a diameter of 0.92 m and depth of 11.5 m. The statnamic test shaft and most of the static load test shafts were constructed using a drilling slurry. Reinforcement consisted of 12 #11 longitudinal bars (3.5 cm diameter) with 7.6 cm (3 inches) of cover. The concrete had a compressive strength of approximately 31 MPa (4500 psi). The lateral load was applied at approximately 30 cm above the ground surface in all tests.

Instrumentation during the statnamic test included strain measurements on both the compression and tension sides of the shaft at each of 6 elevations. Strain measurements were obtained using electrical resistance type strain gauges mounted on #4 sister bars which were tied into the rebar cage. Each sister bar had a pair of T-rosette gauges connected to form a full bridge circuit on each bar, with a gauge factor of 2.6. These gauges were observed to be very stable, with a resolution of less than 1/2 microstrain.

Below-grade instrumentation also included accelerometers at 3 elevations below the surface (plus one atop the shaft). These accelerometers were placed within inclinometer casings by attaching the gauge to an aluminum mount with spring-loaded wheels designed to fit into the grooves in the casing. In this manner the gauges could be placed at any desired elevation and retrieved after completion of the test. For the relatively low accelerations below grade during the statnamic lateral load test (measured to be less than 5 g's), these accelerometer mounts worked quite well. Numerical integration of the accelerometer measurements provide a measure of displacements at depth. For the shafts used in the static lateral tests, the inclinometer casings were used to measure displacement below grade with a conventional inclinometer device.

Measurements at the top of the shaft during the statnamic loading include load,

displacement, and acceleration. Load is measured with a calibrated load cell which is placed between the statnamic piston and a hemispherical bearing on the shaft. Displacement is measured directly using a laser target that senses a remote laser beam; the laser is positioned on the ground surface a sufficient distance from the test shaft so that any ground motion arrivals at the laser itself will not occur within the duration of the test measurements (about 1/4 sec.). An accelerometer on the top of the shaft provides a direct measure of acceleration and, through numerical integration, a redundant measure of displacement of the top of the shaft.

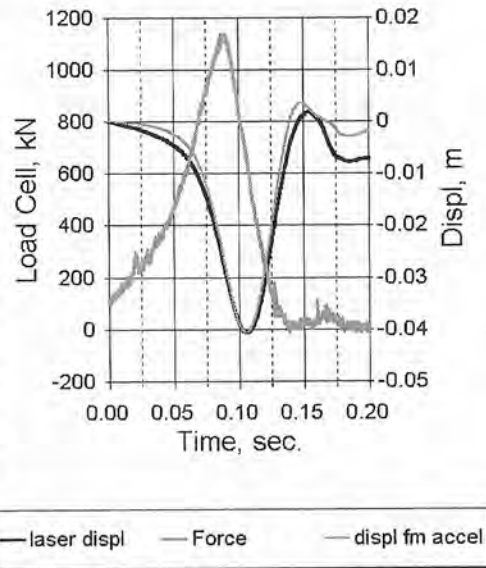


Figure 2 Statnamic Force and Displacement

All instrumentation was monitored with a Megadac® data acquisition system which was programmed to record all data channels at approximately 1 msec intervals.

Test Results

The statnamic loading produced a load and displacement time history as illustrated on Figure 2. The duration of the load pulse is slightly larger than 0.1 seconds with a maximum applied force of 1.1 MN and a maximum displacement of approximately 40 mm. The displacement data suggest that the shaft rebounded with little permanent set and with very little observable oscillation after the initial loading (i.e., the vibration damped out very rapidly).

Measurements of maximum and minimum strain

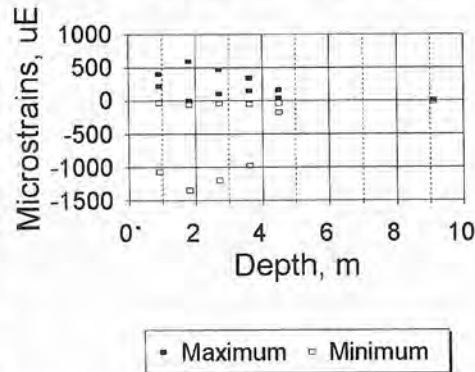


Figure 3 Strain Gauge Peak Values

values at each gauge location are presented on Figure 3; the upper and lower bounds of this figure represent the maximum compressive and tensile strains measured during the test. The maximum bending moment is clearly indicated at a depth of around 2 m. The maximum tensile strains at this level (nearly 1500 microstrains) exceed the maximum compressive strains by a factor of almost 3, suggesting that the shaft was quite severely cracked by this loading. Bending strains below a depth of 4 m are very small.

The downhole accelerometer measurements were integrated to obtain displacement, and these are presented on Figure 4. The peak

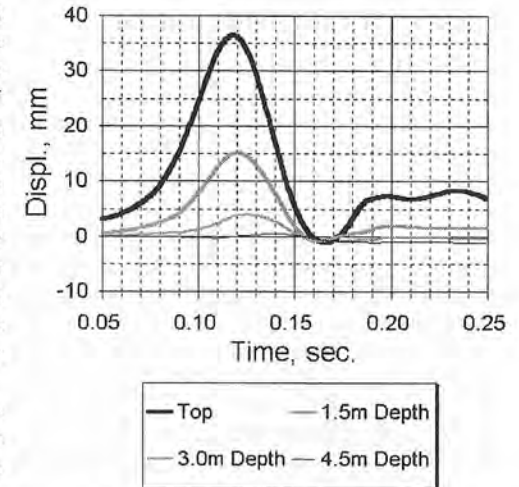


Figure 4 Displacement from Downhole Accel's.

data are seen to exhibit very small phase shifts, thus revealing that wave propagation effects during the statnamic loading are very small.

The loading produces a displacement pattern more analogous to that of a rapid static test due to the low frequency relative to the natural frequency of the shaft. The peak values of displacements as a function of depth below grade are presented on Figure 5. These data indicate that the displacements were concentrated within the upper 3 m of the shaft,

and thus the soil resistance within that region would be expected to dominate the behavior.

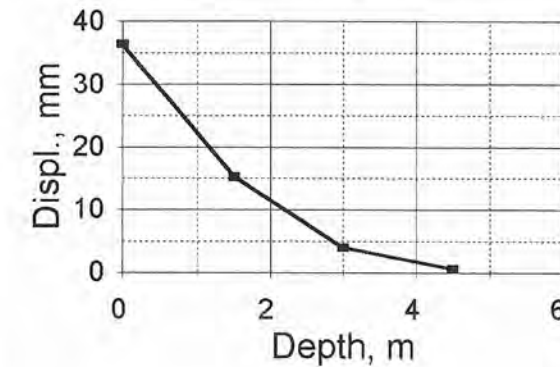


Figure 5 Peak Displ. vs Depth During Statnamic Test

Analysis and Interpretation

A method of evaluating the results of the statnamic lateral test consists of a simple single degree of freedom dynamic model of the following form:

$$F_{\text{statnamic}} = F_{\text{inertia}} + F_{\text{damping}} + F_{\text{static}}$$

where,

- $F_{\text{statnamic}}$ = measured force on the statnamic load cell
- F_{inertia} = inertial resistance from effective mass of the foundation
- F_{damping} = effective viscous damping resistance
- F_{static} = effective static soil resistance

The inertial resistance is roughly that of a cylinder rotating about its base, with a diameter equal to that of the shaft and a height taken as approximately 3 m, based on the observed displacement pattern. For such a cylinder of radius r , height h , and mass m , the mass moment of inertia about the base, I_y is:

$$I_y = m (r^2/4 + h^2/3) = 14.91 \text{ kN-s}^2/\text{m for } 24 \text{ kN/m}^3 \text{ concrete}$$

The rotational acceleration of such a cylinder in relation to a displacement x at the top would be \ddot{x}/h and thus summing moments about the base,

$$(F_{\text{inertia}})h = (I_y)(\ddot{x}/h)$$

therefore, $F_{\text{inertia}} = (I_y/h^2)\ddot{x} = m_e\ddot{x}$

where m_e may be thought of as the effective mass for the foundation. For this test, m_e would be calculated to be 1.66 kN-s²-m. In reality, there is undoubtedly a mass of soil accompanying the shaft as the passive wedge of soil is displaced, so this mass might rationally be increased by a factor of 2 or so.

The damping resistance is presumed to be represented by a viscous damper in which the force F_{damping} is proportional to velocity, \dot{x} , by a constant, c (which is in units of force-sec./length). In order to relate this more meaningfully to a system damping parameter, the damping constant is expressed as a percent of the critical damping, c_c , by

$$D = c/c_c = c/[2(k_s m_e)^{1/2}]; \text{ where } k_s = \text{initial static stiffness}$$

thus, $F_{\text{damping}} = c \dot{x} = D[2(k_s m_e)^{1/2}] \dot{x}$

The static resistance is modeled as a function of displacement, x , using a spring with stiffness k_s . Because the soil response for lateral loading at large strains is known to be highly nonlinear, this spring is modeled as a nonlinear stiffness which decreases as a function of displacement. For the analyses in this paper, the stiffness has been presumed to decay exponentially from an initial value k_i at $x=0$ to a value $k=\alpha k_i$ at a displacement of 5% of the shaft diameter (or $0.1r = 0.046 \text{ m}$ in this case). Thus the

static resistance is modeled using two constants, k_i and α according to:

$$F_{\text{static}} = \exp\{\text{Ln } k_i + \text{Ln}[\alpha(.1r)]\}$$

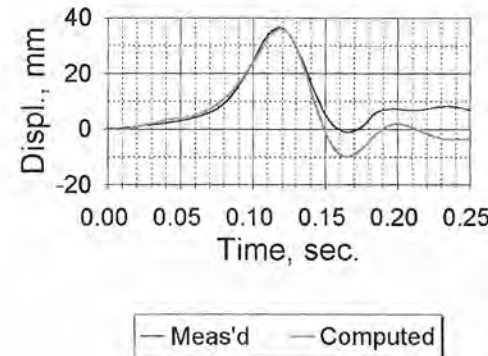


Figure 6 Measured & Model Displ. time history

types of dynamic loadings. For this test, the match shown on Figure 6 was obtained using $m_e = 3.26$, $D = 33\%$, $k_i = 75 \text{ MN/m}$ and $\alpha = 0.25$. The match is observed to be most sensitive to static stiffness. Note that in Figure 6 the measured displacement response indicates some permanent set which is not present in the model; the model does not include a provision for nonlinear unloading and permanent set, so this deviation is not considered particularly important. The unloading stiffness for this simple model was taken as the stiffness at the maximum displacement, so the hysteresis in the unloading response is not simulated.

With the derived computational model, the individual force components contributing to resistance can be estimated as illustrated on Figure 7. Some differing matches were developed using the data presented in Figure 6 in order to evaluate

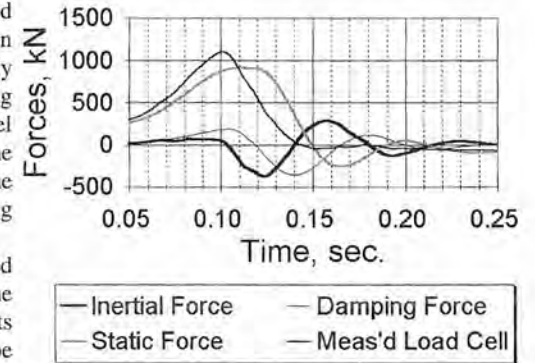


Figure 7 Computed Static and Dynamic Forces

sensitivity to the input parameters. A fairly reasonable match can be achieved with slightly different values of damping resistance and effective mass, but in no case did this result in substantial differences in the derived static forces. The derived forces are presented as a function of displacement (in a manner similar to a static loading test) on

Figure 8. This figure graphically illustrates the nonlinearity in the static component of the resistance, and the relatively small contributions of inertia and damping.

Comparison with Conventional Static Tests

Five shafts which were similar to the statnamic test shaft were subjected to static lateral loading tests. These shafts exhibited a significant variability, illustrating the sensitivity of laterally loaded deep foundations to variations in near-surface soil characteristics. The load - displacement response for the five static tests are shown on Figure 9, along

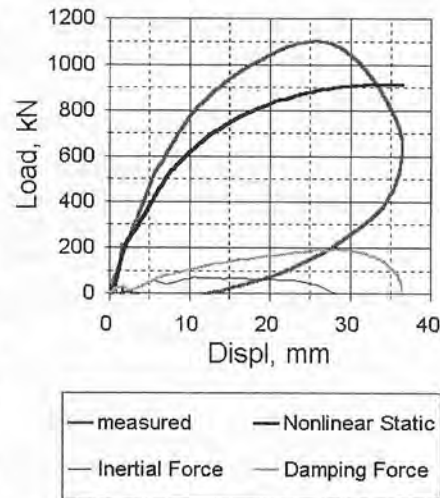


Figure 8 Derived Force - Displacement Response

with the derived nonlinear static component of force from the statnamic test shaft.

These data reveal that, besides the inherent variability in the lateral stiffness at the site, there appears to be a significant rate effect for this foundation even after accounting for inertia and damping with this simple model. The initial stiffness at small displacements match fairly well, and it appears that the forces achieving large displacements trend toward a consistent relationship. Within the 10 to 30 mm displacements (1 to 3% of the shaft diameter), the stiffness derived from statnamic testing is greater. A large portion of this difference may be attributed to rate effects in the reinforced concrete as this

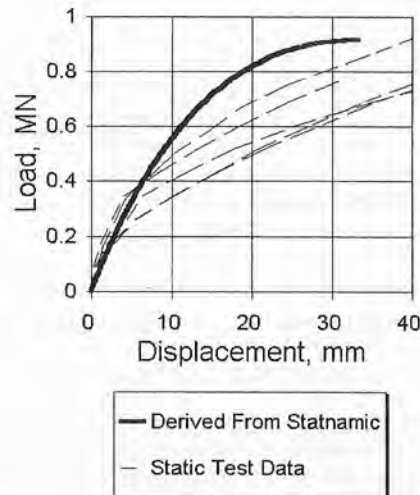


Figure 9 Static & Derived Load vs Displ

is the region in which cracking and nonlinear bending response (EI) in the shafts occur. According to data presented by Tedesco, McDougal and Ross (1999), the tensile strength of the concrete at strain rates typical of those during the statnamic test is on the order of 2 to 2.5 times higher than for static testing. This increased stiffness (EI) in the test shaft may account for much of the difference between the statnamic and static loading data presented on Figure 9. Rate effects in soil shearing resistance may also contribute. These data also suggest that for transient loadings in which rate effects might be important, designers using simple static p-y models for design may be conservative as there may be additional resistance unaccounted for in a model based on simple static load tests.

Future Research

Additional research with statnamic lateral testing is planned, with several key elements identified:

- 1) repeated lateral statnamic testing with several progressively increasing load levels may help to construct a nonlinear load vs displacement relationship with greater reliability in the derived forces across a range of displacement amplitudes,
- 2) lateral statnamic testing on linear elastic steel piles is planned, and these tests will eliminate the nonlinearity inherent in reinforced concrete members in bending and allow a more focused attention on soil nonlinearity,
- 3) the lateral statnamic test data will be analyzed using dynamic p-y curves in which the variation of soil resistance with depth can be accounted for and the additional damping resistance in the soil response "calibrated" with large scale and large amplitude dynamic test results,
- 4) repeated lateral statnamic testing at constant load levels so as to obtain data which can be used to calibrate the gapping around the piles and hysteresis with dynamic p-y curves
- 5) testing of groups of steel piles in which dynamic pile-soil-pile interaction is a factor.

Acknowledgements

The author wishes to acknowledge the contributions to this research of the Morris-Shea Bridge Company, the Alabama DOT, Applied Foundation Testing, Inc., the Federal Highway Administration, Professor Gray Mullins of the University of South Florida, and the Auburn University Highway Research Center. The author wishes to express a special appreciation to Professor Lymon Reese for his many years of help and guidance and interest in lateral load testing and in who's honor this paper is presented.

References

Tedesco, J.W., W.G. McDougal, and C.A. Ross, 1999. Structural Dynamics, Theory and Applications, Addison Wesley Longman, Inc., Menlo Park, Calif., 869 p.

Vinson, J.L. and D.A. Brown, 1997. "Site Characterization of the Spring Villa Geotechnical Test Site and a Comparison of Strength and Stiffness Parameters for a Piedmont Residual Soil," Highway Research Center Report No. IR-97-04, Nov., 1997, 385pp.

Subject Index

Page number refers to the first page of paper

- Axial loads, 61, 180
- Bearing capacity, 96, 180, 296
- Boring, 135
- Caissons, 247, 281
- Calcareous soils, 17
- Cohesive soils, 296
- Collapse, 76
- Computation, 115
- Concrete piles, 296
- Concrete, prestressed, 296
- Constitutive models, 37
- Construction methods, 196
- Deep foundations, 1, 115, 196, 216, 281
- Deep water, 216, 247
- Design, 1, 96, 135
- Differential settlement, 96
- Displacement, 150
- Drilled shafts, 180, 309
- Drilling, 196
- Driven piles, 180, 216
- Dynamic response, 165
- Experimentation, 17
- Finite element method, 37
- Foundations, 37, 309
- Full-scale tests, 309
- Geology, 135
- Gulf of Mexico, 247, 281
- Installation, 196, 216, 261
- Interactions, 261
- Lateral loads, 17, 61, 309
- Limit analysis, 76
- Liquefaction, 37, 165
- Load transfer, 17, 61
- Numerical models, 234
- Offshore structures, 1, 76, 135, 234
- Parallel processing, 115
- Performance, 196
- Pile bearing capacities, 261
- Pile driving, 216
- Pile foundations, 61, 76, 165, 261
- Pile groups, 150
- Pile load tests, 261, 296
- Piles, 17, 96, 135, 234, 261
- Plasticity, 76
- Predictions, 180
- Raft foundations, 96
- Reliability, 135
- Reliability analysis, 180
- Seismic effects, 165
- Settlement analysis, 96
- Soil resistance, 234, 309
- Soil-pile interaction, 61
- Soils, 150
- Soil-structure interaction, 37
- Static tests, 296
- Strain gages, 309
- Stress analysis, 247
- Suction, 234, 247, 281
- Three-dimensional analysis, 115
- Trends, 1
- Vibration effects, 196
- Yield surface, 76